STAT3 as a Potential Target for Tumor Suppressive Effects of 15-Deoxy-$\Delta^{12,14}$-prostaglandin J$_2$ in Triple Negative Breast Cancer

Su-Jung Kim[1], Nam-Chul Cho[2], Young-Il Hahn[3], Seong Hoon Kim[1], Xizhu Fang[1], Young-Joon Surh[1,3,4]

[1]Research Institute of Pharmaceutical Sciences, College of Pharmacy, Seoul National University, Seoul, [2]Korea Chemical Bank, Korea Research Institute of Chemical Technology, Daejeon, [3]Department of Molecular Medicine and Biopharmaceutical Sciences, Graduate School of Convergence Science, Seoul National University, [4]Cancer Research Institute, Seoul National University, Seoul, Korea

STAT3 plays a prominent role in proliferation and survival of tumor cells. Thus, STAT3 has been considered to be a prime target for development of anti-cancer therapeutics. The electrophilic cyclopentenone prostaglandin,15-deoxy-$\Delta^{12,14}$-prostaglandin J$_2$ (15d-PGJ$_2$) has been well recognized for its capability to modulate intracellular signaling pathways involved in cancer cell growth and progression. We previously reported that 15d-PGJ$_2$ had potent cytotoxicity against harvey-*ras* transformed human mammary epithelial cells through direct interaction with STAT3. In this study, we have attempted to verify the inhibitory effects of 15d-PGJ$_2$ on STAT3 signaling in human breast tumor cells. The triple negative breast cancer cell lines, MDA-MB-231 and MDA-MB-468 displaying constitutive phosphorylation of STAT3 on the tyrosine 705 (Tyr705) residue, underwent apoptosis upon inhibition of STAT3 by 15d-PGJ$_2$. In contrast, estrogen receptor positive MCF-7 breast cancer cells that do not exhibit elevated STAT3 phosphorylation were much less susceptible to 15d-PGJ$_2$-induced apoptosis as assessed by PARP cleavage. Furthermore, 15d-PGJ$_2$ inhibited interleukin-6-induced tyrosine phosphorylation of STAT3 in LNCaP cells. According to molecular docking studies, 15d-PGJ$_2$ may preferentially bind to the cysteine 259 residue (Cys259) present in the coiled-coil domain of STAT3. Site-directed mutagenesis of STAT3 identified Cys259 to be the critical amino acid for the 15d-PGJ$_2$-induced apoptosis as well as epithelial-to-mesenchymal transition. Taken together, these findings suggest STAT3 inactivation through direct chemical modification of its Cys259 as a potential therapeutic approach for treatment of triple negative breast cancer treatment.

Key Words Breast neoplasms, Cyclopentenone prostaglandin, 15-Deoxy-$\Delta^{12,14}$-prostaglandin J$_2$, STAT3

INTRODUCTION

Breast cancer is the most commonly diagnosed malignancy and the leading cause of cancer-related deaths among women worldwide [1-3]. Breast cancer prevalence is increasing worldwide every year, especially in young women. Therefore, development of efficient therapeutic strategies as well as identification of novel targets for prevention and treatment of breast cancer is clinically important [2].

15-Deoxy-$\Delta^{12,14}$-prostaglandin J$_2$ (15d-PGJ$_2$) is a cyclopentenone prostaglandin (PG) that can act as an endogenous ligand for PPARγ [4,5]. 15d-PGJ$_2$ is characterized by the presence of an α,β-unsaturated carbonyl group in the cyclopentenone ring. Because of this electrophilic moiety, 15d-PGJ$_2$ is capable of forming covalent adducts with some target proteins, thereby altering their structures and biological functions, independently of PPARγ activation [6-9].

Janus kinase (JAK)-STAT axis plays a major role in the regulation of cell cycle progression and proliferation [10]. STAT proteins are a family of latent cytoplasmic transcription factors that become phosphorylated by JAK in response to various cytokines and growth factors. The phosphorylated STAT (P-STAT) undergoes dimerization and translocates into the nucleus where it binds to the promoter of its downstream target genes and induces their transcription. At least seven members of mammalian STAT family proteins have been identified: STAT1, STAT2, STAT3, STAT4, STAT5A, STAT5B, and STAT6, which are encoded by distinct genes.

All STAT proteins consist of an amino acid domain (NH_2), a coiled-coil domain responsible for binding to interactive proteins, a DNA binding domain, a linker domain, a Src homology 2 (SH2) domain required for phosphorylation and dimerization, and a C-terminal transactivation domain [11]. Among STAT family members, persistent activation of STAT3 is frequently observed in many different types of human malignancy, which contributes to the growth and survival of cancer cells [12-15]. The knockdown of the STAT3 by antisense RNA or siRNA resulted in the induction of cancer cell apoptosis and tumor regression [16,17]. Therefore, targeting aberrant STAT3 signaling provides a universal therapeutic strategy for treating a wide variety of human tumors that harbor abnormal STAT3 activity.

15d-PGJ_2 has potent tumor suppressive effects against breast, prostate and colorectal cancer [18-20]. It induces apoptosis by reactive oxygen species-mediated inactivation of Akt in colorectal cancer cells [21]. 15d-PGJ_2 inhibits constitutive NF-κB activities in chemotherapy-resistant estrogen receptor (ER)-negative breast cancer cells, which accounts for induction of their apoptosis [22]. Furthermore, 15d-PGJ_2 induced apoptosis of cancer cells by modulating expression levels of the Bcl-2 family member proteins, such as Bax and Bcl-2 [23,24]. It also induces apoptosis of macrophages, fibroblasts, and endothelial cells that constitute tumor microenvironment [25-27].

Several studies revealed an association between 15d-PGJ_2-mediated STAT3 inactivation and induction in cancer cells. 15d-PGJ_2 downregulated expression of genes encoding interleukin-6 (IL-6) and STAT3 while upregulating suppressors of cytokine signaling (SOCS) 3 in TPC-1 human thyroid papillary carcinoma cells [28]. In activated glial cells, 15d-PGJ_2 induces the transcription of SOCS 1 and 3, which in turn inhibits JAK activity [28,29]. We recently reported that 15d-PGJ_2-mediated inactivation of STAT3 through covalent modification which led to apoptosis in H-*ras* transformed human mammary epithelial cells [30]. The present study was aimed to verify the inhibitory effects of 15d-PGJ_2 on oncogenic STAT3 signaling and its mode of action in human breast cancer cells.

MATERIALS AND METHODS

Chemicals
15d-PGJ_2 was purchased from Cayman Chemical Co. (Ann Arbor, MI, USA). Dulbecco's modified Eagle's medium (DMEM)/Ham's nutrient mixture F-12 (1:1) and horse serum were obtained from Gibco BRL (Grand Island, NY, USA). Cholera toxin, hydrocortisone, insulin, human EGF), and MTT were purchased from Sigma-Aldrich Chemicals (St. Louis, MO, USA). P-STAT3-TA-Luc plasmid was supplied from BD Biosciences Clontech (Palo Alto, CA, USA).

Cell culture
The immortalized human mammary epithelial MCF10A and MCF10A cells transformed by an active Ha-*ras* (MCF10A-*ras*) cells were cultured in DMEM/F-12 medium supplemented with 5% heat-inactivated horse serum, 10 μg/mL insulin, 100 ng/mL cholera toxin, 0.5 μg/mL hydrocortisone, 20 ng/mL human EGF, 2 mmol/L L-glutamine, and 100 units/mL penicillin/streptomycin. The human breast cancer cell lines (MDA-MB-231 and MCF-7) were obtained from the Korean Cell Line Bank (Seoul, Korea). The human prostate cells (LNCaP and PC-3) and the human breast cancer cell (MDA-MB-468) were supplied from the American Type Culture Collection (ATCC, Rockville, MD, USA). MDA-MB-231, MDA-MB-468 and LNCaP cells were maintained in DMEM, and MCF-7 and PC-3 cells in RPMI 1640 cell culture media. All culture media were supplemented with 10% (v/v) heat-inactivated FBS (Gibco; Thermo Fisher Scientific, Waltham, MA, USA), 100 U/mL penicillin and 100 g/mL streptomycin. These cell lines were grown at 37ºC in a humidified air/CO_2 (19:1) atmosphere.

MTT reduction assay
Cells were plated at a density of 3×10^4 cells/300 μL in 48-well plates, and the cell viability was determined by the MTT reduction assay. After incubation, cells were treated with the MTT solution (final concentration, 1 mg/mL) for 2 hours. The dark blue formazan crystals formed in intact cells were dissolved with dimethyl sulfoxide, and the absorbance at 570 nm was read using a microplate reader. Results were expressed as the percentage of MTT reduction obtained in the treated cells, assuming that the absorbance of control cells was 100%.

Transient transfection
PC-3 cells were seeded in a six-well dish at a density of 2×10^5 cells per well and grown to 60% to 80% confluence in the complete growth medium. The cells were transfected with plasmid construct harboring the STAT3 wild type (WT) or a mutant form of STAT3 with cysteine 251 (Cys251) or Cys 259 replaced by alanine (C251A/C259A) using WelFect-M GOLD transfection reagent (WelGENE, Gyeongsan, Korea), and the transfection was carried out according to the instructions supplied by the manufacture.

Xenograft assay
Male BALB/c (nu/nu) mice, 6 weeks of age, were purchased from Central Lab Animal Inc. (Seoul, Korea) and were housed in a 12 hours light/12 hours dark cycle and fed rodent chow and water ad libitum. PC-3 cells (1×10^7 in 100 μL PBS) were injected subcutaneously on the right hind flank. Tumor volume (length × width × depth × 0.52) was measured three times a week. Tumor volume was regularly measured with digital calipers and calculated according to the formula: V = 0.5 ab², where 'a' is the longest and 'b' is the shortest perpen-

dicular diameters. After mice were killed, xenograft tumors were excised and fixed in formalin for immunofluorescence or immunohistochemical analysis. All protocols for animal experiments were approved by the Institutional Animal Care and Use Committee (IACUC) of Seoul National University (authorization number: SNU-170810-2-6).

Western blot analysis

Breast cancer cells were lysed in lysis buffer [250 mmol/L sucrose, 50 mmol/L Tris-HCl (pH 8.0), 25 mmol/L KCl, 5 mmol/L MgCl$_2$, 1 mmol/L EDTA, 2 mmol/L NaF, 2 mmol/L sodium orthovanadate, and 1 mmol/L phenylmethylsulfonylfluoride] for 15 minutes on ice followed by centrifugation at 12,000 ×g for 20 minutes. The protein concentration of the supernatant was measured by using the bicinchoninic acid protein assay (Pierce Biotechnology, Inc.). Protein (30 μg) was separated by running through 8% SDS PAGE gel and transferred to the polyvinylidene fluoride membrane (Gelman Laboratory, Ann Arbor, MI, USA). The blots were blocked with 5% nonfat dry milk PBST buffer (PBS containing 0.1% Tween-20) for 1 hours at room temperature. The membranes were incubated for 2 hours at room temperature with 1:1,000 dilution of one of the antibodies against N-cadherin (Santa Cruz Biotechnology, Santa Cruz, CA, USA), β-actin (Santa Cruz Biotechnology), E-cadherin (BD Bioscience, San Jose, CA, USA), P-STAT3^{Y705} (Cell Signaling Technology, Beverly, MA, USA), STAT3 (Cell Signaling Technology), or PARP (Cell Signaling Technology). The blots were rinsed three times with PBST buffer for 10 minutes each. Washed blots were treated with 1:5,000 dilution of the horseradish peroxidase conjugated-secondary antibody (Pierce Biotechnology, Inc., Waltham, MA, USA) for 1 hour and washed again three times with PBST buffer. The transferred proteins were visualized with an enhanced chemiluminescence detection kit (Amersham Pharmacia Biotech, Amersham, UK).

Immunoprecipitation

For co-immunoprecipitation experiments, cells were lysed in immunoprecipitation buffer [20 mM Tris–HCl (pH 7.5), 150 mM NaCl, 1 mM Na 2 EDTA, 1 mM EGTA, 1% Triton, 2.5 mM sodium pyrophosphate, 1 mM β-glycerophosphate, 1 mM Na$_3$VO$_4$, 1 μg/mL leupeptin and protease inhibitors] (Cell Signaling Technology). On the following day, samples were added to 50 μL A/G-agarose beads (Santa Cruz Biotechnology) and rotated for 2 hours at 4°C. Protein A/G-agarose beads were washed four times with buffer A (10 mM HEPES pH 7.9, 60 mM KCl, 2 mM EDTA, 1 mM EGTA, 0.1% Triton X-100, 1 mM dithiothreitol, and protease and phosphatase inhibitors). Immunocomplexes were resolved on SDS PAGE, transferred to polyvinylidene fluoride membranes and analyzed with immunoblotting.

Molecular docking study

A molecular docking study was carried out using Schroding-

er packages v9.5 (Schrödinger, LLC, New York, NY, USA). STAT3 crystal structures were retrieved from PDB bank (PDB code: 1BG1) [31,32]. Protein structures were prepared with the standard procedure of the Protein Preparation Wizard module. STAT3 protein was protonated at neutral pH, and hydrogen atoms were refined by energy minimization. The LigPrep module was used from the Maestro suite to generate a 3D structure of the ligands by adding hydrogen atoms and removing salt and ionizing at pH 7.4. The grid box was automatically determined within 5.0 Å of the Cys259 residue. The reaction type for covalent bonding was set to Michael addition. Binding energy on the 10 STAT3-15d-PGJ$_2$ complexes was calculated after minimization of residues within 3 Å of ligand using Prime MM-GBSA. A binding pose with low Prime ΔG$_{bind}$ was selected for analysis.

Kaplan–Meier analysis

Kaplan–Meier analysis of the STAT3 genes in 902 breast cancer patient database (including all molecular subtypes or ER-positive or ER-negative) was performed using Kaplan–Meier Plotter (http://kmplot.com/analysis/index.php?p=service&default=true).

Gene Set Enrichment Analysis (GSEA)

Data sets of breast invasive carcinoma of The Cancer Genome Atlas (TCGA) were downloaded using TCGAbiolink [33] in R. Eight hundred seventy four primary BRCA breast invasive carcinoma samples were categorized into two groups, namely a high and low-expression group based on the 75% cut-off value of The P-STAT3 level from protein expression data [reverse phase protein array (RPPA)]. Normalized mRNA expression data of each 218 sample in high and low groups were retrieved. GSEA was conducted to explore potential biological processes and pathways by using the MSigDB database. Gene set enrichment was performed by the difference of class for the categorical phenotype to calculate fold change. Other options were set to default. Gene sets less than 0.01 of a nominal P-value and 0.05 of false discovery rate were chosen as statistically significance.

Statistical analysis

In necessary, data were expressed as means ± SDs of at least three independent experiments, and statistical analysis for a single comparison was performed using the Student's t-test. The criterion for statistical significance was $P < 0.05$.

RESULTS

STAT3 is upregulated in breast cancer tissues which predicts a poor prognosis in breast cancer patients

To determine the role for STAT3 in breast cancer, we first analyzed the expression of STAT3 in invasive ductal carcinoma

and non-tumor tissues from the tissue array. We found that STAT3 was significantly upregulated in breast cancer tissues, compared to adjacent normal tissues (Fig. 1A). GSEA was conducted using RNA-seq and RPPA data set of TCGA databases to explore potential biological processes and pathways in STAT3 overactivating breast cancers. The 75% cut-off value of P-STAT3 levels in RPPA was used to categorize patients with breast invasive carcinoma into low- and high-level

groups. GSEA reveals that enriched pathways positively associated with STAT3 activation were KRAS signaling, hypoxia, and inflammatory responses, while the negatively correlated pathways include DNA repair and G2M-checkpoint (Fig. 1B). We further explored the prognostic implication of STAT3 in breast cancer. Kaplan–Meier survival analysis revealed that patients with a high level of STAT3 expression had significantly shorter recurrence-free survival time (Fig.
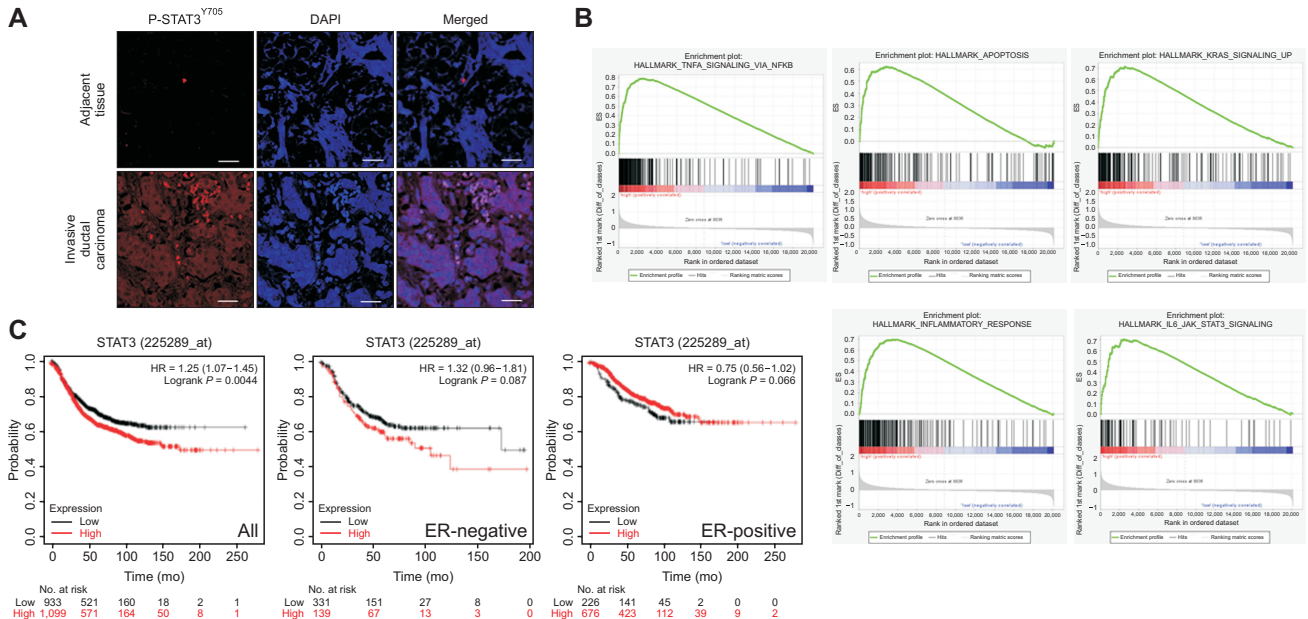

Figure 1. P-STAT3^{Y705} expression and survival prognosis. (A) The expression of P-STAT3^{Y705} in invasive ductal carcinoma and adjacent normal tissues was measured by immunofluorescent staining of a tissue array. Scale bar, 200 μm. (B) Gene Set Enrichment Analysis (GSEA) demonstrates the regulation of the STAT3 signaling in breast cancer tissues by phosphorylation level of STAT3. (C) STAT3 expression correlates with poor survival in breast cancer data set. Patients were further identified as high and low STAT3 expression subgroups. P-STAT3, phosphorylated STAT3; ES, enrichment score; IL6, interleukin 6; JAK, Janus kinase; HR, hazard ratio; ER, estrogen receptor.
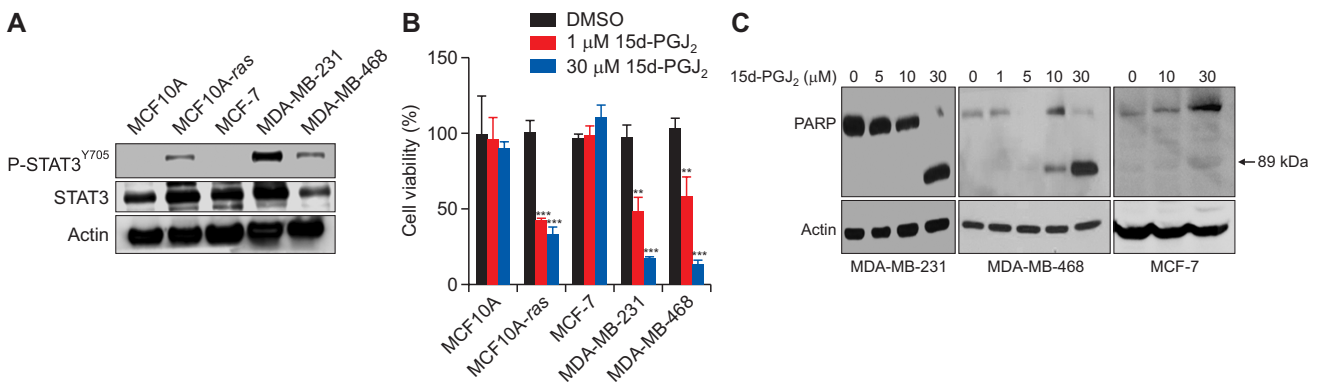

Figure 2. 15-deoxy-Δ^{12,14}-prostaglandin J$_2$ (15d-PGJ$_2$)-induced apoptosis of breast cancer cells. (A) Differential P-STAT3^{Y705} expression in breast cancer cell lines. The basal levels of P-STAT3^{Y705} in MCF10A-*ras*, MCF-7, MDA-MB-231 and MDA-MB-468 cells as well as a non-oncogenic human breast epithelial MCF10A cell line were assessed by Western blot analysis. (B) MCF10A, MCF10A-*ras*, MCF-7, MDA-MB-231, and MDA-MB-468 cells were exposed to 15d-PGJ$_2$ (10 or 30 μM) for 24 hours. The cellular viabilities were determined by the MTT assay. The values represent mean ± SD of the three independent experiments. DMSO, Dimethyl sulfoxide. **$P < 0.01$; ***$P < 0.001$ versus the corresponding control. (C) 15d-PGJ$_2$ induces apoptosis in human breast cancer cell lines. Western blot analysis was performed with lysates from MDA-MB-231, MDA-MB-468 and MCF-7 cells after 24-hour treatment with 15d-PGJ$_2$.

1C) compared with those with a low level of STAT3 expression in ER-negative breast cancer.

15d-PGJ$_2$ inhibits the growth of the human breast carcinoma cells harboring constitutively activated STAT3

We also compared the STAT3 signaling in representative human breast cancer cell lines with different ER status. As illustrated in Figure 2A, ER-negative MDA-MB-468 and MDA-MB-231 cells displayed a greater extent of STAT3 activation than the ER-positive MCF-7 cells as evidenced by enhanced STAT3 tyrosine 705 (Tyr705) phosphorylation. MCF10A-*ras* also express P-STAT3 whilst it is barely detectable in the non-oncogenic MCF10A parental line. In line with these findings, 15d-PGJ$_2$ treatment resulted in a concentration-dependent decrease in the viability of MDA-MB-231, MDA-MB-468 and MCF10A-ras cells, but not in MCF10A and MCF-7 cells (Fig. 2B). Moreover, 15d-PGJ$_2$ at 30 μM induced apoptosis in the MDA-MB-231 and MDA-MB-468 cells at 30 μM. However, this was not prominent in the ER-positive MCF-7 cells (Fig. 2C).

15d-PGJ$_2$ inhibits the constitutive and inducible phosphorylation of STAT3

We further examined whether the anti-proliferative and proapoptotic activities of 15d-PGJ$_2$ were associated with suppression of STAT3 activation in MDA-MB-231 and MDA-MB-468 cells. Treatment of these cell lines with 15d-PGJ$_2$ concentration dependently reduced P-STAT3 levels (Fig. 3A and 3B). In addition, 15d-PGJ$_2$ also effectively inhibited IL-6-induced phosphorylation of STAT3 and the STAT3 target protein, cyclin D1 in the LNCaP prostate cancer cell line expressing a relatively low level of constitutively active STAT3 (Fig. 3C). Consistent with these observations, IL-6-induced STAT3 transcriptional activity measured by the luciferase reporter gene assay was diminished by 15d-PGJ$_2$ treatment (Fig. 3D). As STAT3 Tyr705 phosphorylation is known to facilitate STAT3 dimerization, we analyzed whether 15d-PGJ$_2$ inhibited STAT3 dimerization by using the co-immunoprecipitation assay. For this experiment, we transfected PC-3 cells with hemagglutinin (HA)- and Myc-tagged STAT3. As shown in Figure 3E, 15d-PGJ$_2$ markedly suppressed the dimerization of exogenous STAT3 (Fig. 3E).

The electrophilic β-carbon in an α,β-unsaturated carbonyl group can react with electron-rich nucleophiles, forming a covalent bond via the Michael addition reaction. 15d-PGJ$_2$ harboring such reactive moiety can covalently bind to nucleophilic cysteinyl thiol group(s) of diverse cellular proteins [34]. The STAT3 protein is composed of 6 functional domains (Fig. 4A), among which the coiled-coil domain is the most
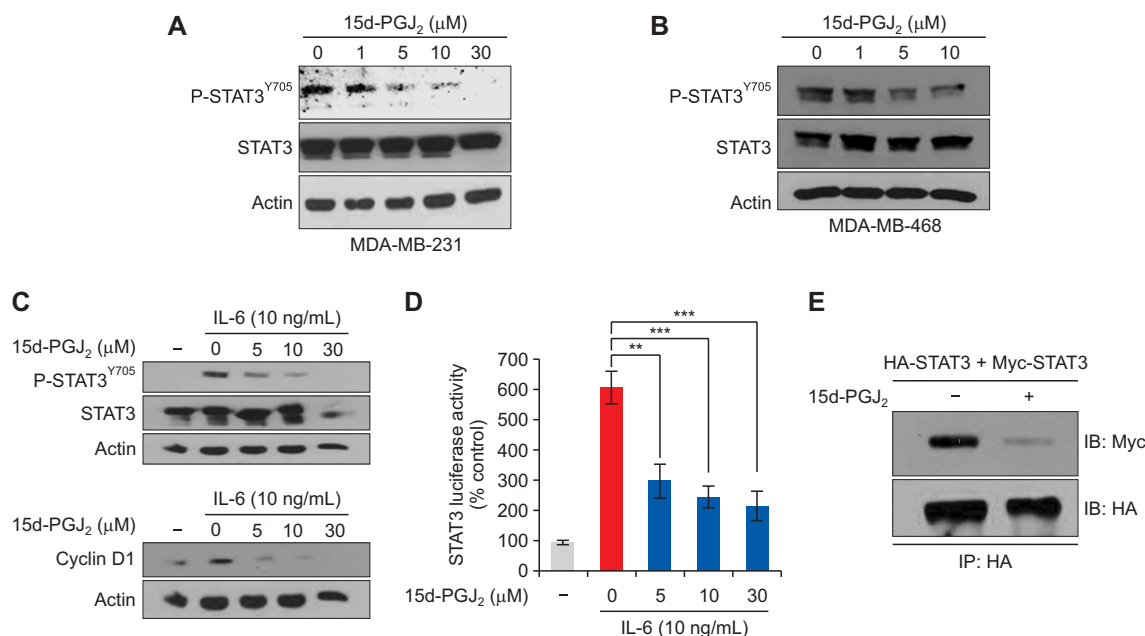

Figure 3. 15d-PGJ$_2$-mediated inactivation of STAT3 through inhibition of STAT3 dimerization. (A, B) Whole extracts were prepared and examined by immunoblotting for P-STAT3^{Y705}, STAT3 and β-actin in MDA-MB-231 and MDA-MB-468 cells. (C) LNCaP prostate cancer cells were pre-incubated in 15d-PGJ$_2$ (5, 10, 30 μM) for 5 hours and treated in interleukin-6 (IL-6) (10 ng/mL) for 16 hours. Whole extracts were prepared and examined for P-STAT3^{Y705}, STAT3, cyclin D1 and β-actin by immunoblot analysis. (D) Luciferase activity was measured with LNCaP cells preincubated with indicated concentrations of 15d-PGJ$_2$ for 5 hours and then stimulated with IL-6 for 16 hours. **$P < 0.01$; ***$P < 0.001$. (E) PC-3 cells were co-transfected with HA-tagged STAT3 and Myc-tagged STAT3 and treated with 15d-PGJ$_2$ for 24 hours. The total lysates obtained from the transfected cells were immunoprecipitated with anti-HA antibody and analyzed by Western blotting with anti-Myc or anti-HA antibody. 15d-PGJ$_2$, 15-deoxy-Δ^{12,14}-prostaglandin J$_2$; P-STAT3, phosphorylated form of STAT3; IL-6, interleukin-6; IP, immunoprecipitation; HA, hemagglutinin; IB, immunoblotting.
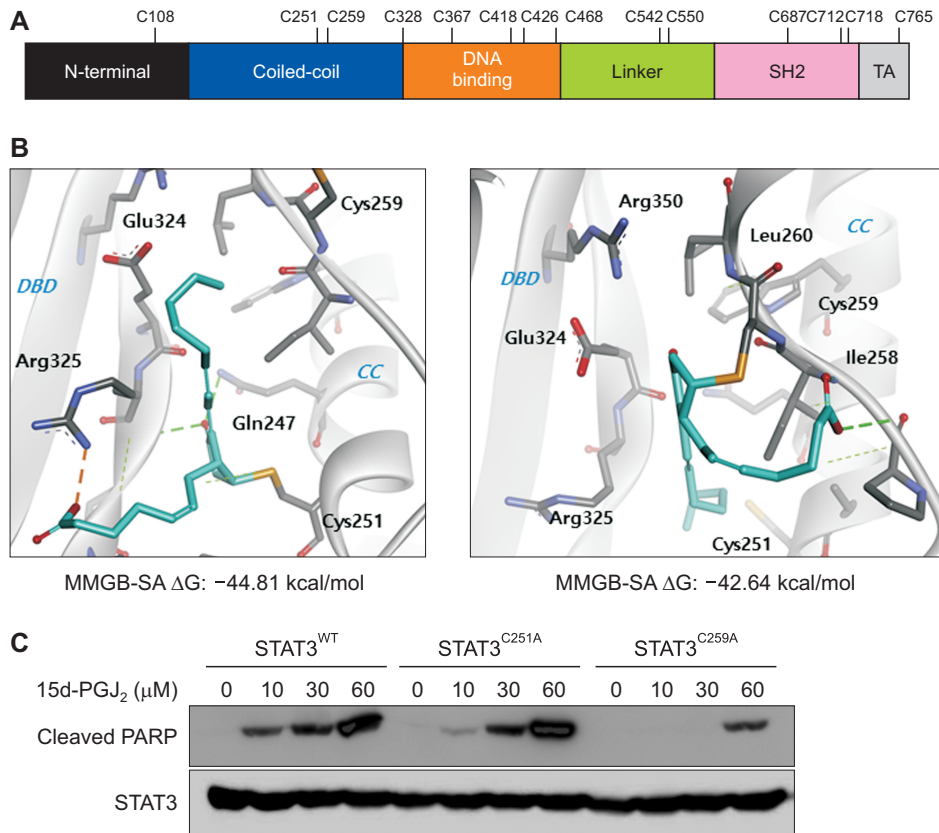
Figure 4. Cysteine 259 residue of STAT3 as a putative binding site of 15-deoxy-$\Delta^{12,14}$-prostaglandin J$_2$ (15d-PGJ$_2$). (A) Cysteine residues present in human STAT3. The STAT3 protein consists of 770 amino acids and is divided into 6 distinct functional domains: the N-terminal domain, coiled-coil domain, DNA-binding domain, a linker domain, Src homology 2 (SH2) domain, and C-terminal transactivation domain. (B) Covalent binding of 15d-PGJ$_2$ to STAT3 as predicted by computational modeling. Schrodinger program was used in docking analysis for 15d-PGJ$_2$ interaction with cysteine 251 and 259 of STAT3 as described in Materials and Methods. (C) PC-3 cells were transiently transfected with GFP-tagged WT STAT3 (STAT3^{WT}) or GFP-tagged mutant STAT3 (STAT3^{C251A} or STAT3^{C259A}) followed by 15d-PGJ$_2$ treatment for 24 hours. The cleaved PARP was detected by Western blot analysis. SH2, Src homology 2; TA, transactivation; DBD, DNA-binding domain; CC, coiled-coil domain; MMGB-SA ΔG, binding free energy calculated with Molecular Mechanics with Generalized Born and Surface Area.

critical region for STAT3 recruitment to the receptor and the subsequent tyrosine phosphorylation and tyrosine phosphorylation-dependent activities, such as dimer formation, nuclear translocation, and DNA binding [35,36]. Notably, a short region in the first α-helix of the coiled-coil domain and a portion of the DNA-binding domain of STAT3 interact with another transcription factor, c-Jun, which facilitates the IL-6-inducible a2-macroglobulin gene transcription [37].

As part of our initial studies to identify potential binding sites of 15d-PGJ$_2$ for STAT3, we conducted molecular docking simulation to predict the mode of interaction between 15d-PGJ$_2$ and selected cysteine residues of STAT3. Covalent docking results show that 15d-PGJ$_2$ may stably bind to the interface of the DNA binding domain and the coiled-coil domain of STAT3 near cysteine 251 and cysteine 259 residues with –44.81 kcal/mol and –42.64 kcal/mol, respectively of binding free energy calculated with Molecular Mechanics with Generalized Born and Surface Area (MM-GBSA ΔG). On docking poses of 15d-PGJ$_2$ with Cys251 and Cys259 residues, its

carboxyl group is predicted to form hydrogen bonds with Arg325 and Ile258 residues, respectively and an aliphatic chain lies and occupies a cavity of binding pocket (Fig. 4B).

To find out which of the two putative cysteines are likely to be preferred for covalent interaction with 15d-PGJ$_2$, we mutated both amino acids to alanine and analyzed the effects of these mutations on the 15d-PGJ$_2$-induced PARP cleavage. The PC-3 cell line bears a STAT3 whole gene deletion mutation on chromosome 17. Therefore, this STAT3-null cell line is useful for studying the effects of ectopic overexpression of STAT3 and its mutant constructs, especially by excluding the effects of endogenous STAT3. As breast cancer cells we used in this study express endogenous STAT3, we utilized this PC-3 cells as a tool to more precisely assess the comparative effects of ectopically overexpressed STAT3 and its cysteine-alanine mutant forms.

In PC-3 cells transiently transfected with cysteine 251-mutated STAT3 (STAT3^{C251A}), 15d-PGJ$_2$-induced PARP cleavage was almost equivalent to that observed in the cells express-

ing wild type STAT3 (STAT3^{WT}) (Fig. 4C). However, substitution of Cys259 with Ala (STAT3^{C259A}) resulted in marked reduction in the PARP cleavage following 15d-PGJ$_2$ treatment (Fig. 4C).

STAT3 C259A mutation attenuates epithelial-to-mesenchymal transition (EMT) and xenograft tumor growth

EMT is an essential feature of invasive and metastatic cancer. During EMT, cells undergo morphological changes with enhancement of motility [38,39]. Loss of epithelial marker expression and a concomitant increase in the expression of mesenchymal markers are the characteristic events of EMT [38,40]. The contribution of intracellular signaling components to the induction of EMT through activation of the JAK/STAT3 signaling in cancer progression has been reported [41].

Enforced expression of STAT3^{C259A} caused a shift in cell morphology from mesenchymal to a more epithelial phenotype, with increased cell-to-cell contact and loss of cell spreading (Fig. 5A). Further, we showed that cysteine 259-mutated STAT3 cells expressed a higher level of the typical epithelial marker, E-cadherin and a lower level of the mesenchymal marker, N-cadherin than did the WT STAT3 cells (Fig. 5B).

The critical role of Cys259 in oncogenic functions of STAT3 was also assessed in vivo by using a mouse xenograft breast tumor model in which green fluorescent protein (GFP)-tagged

STAT3^{WT}- or STAT^{C259A}-overexpressing PC-3 cells were transplanted into athymic nude mice. While tumors derived from wild type cells were continuously growing for 27 days, those from cells harboring STAT3^{C259A} showed a slower growth rate (Fig. 5C). Moreover, the infiltrating number of STAT3-expressing cells in tumor tissues was significantly reduced by Cys259 mutation (Fig. 5D). Immunohistochemical analysis revealed that tyrosine P-STAT3^{Y705} are downregulated in STAT3^{C259A} compared with STAT3^{WT}expressing tumors (Fig. 5E).

The above findings, taken all together, indicate that the Cys259 residue of STAT3 is essential for its function as a transcription factor, and suggest that covalent modification of this amino acid by 15d-PGJ$_2$ mimics mutation at the same site which may provoke a similar impact.

DISCUSSION

PPARγ activation has been linked to cell growth inhibition and induction of apoptosis in several types of human cancer [18-20]. 15d-PGJ$_2$, initially discovered as an endogenous ligand for PPARγ, has anti-cancer properties [42]. 15d-PGJ$_2$ induces apoptosis of some cancer cells [20-24,28,43,44]. However, its tumor suppressive effects are not necessarily mediated through activation of PPARγ. For instance, 15d-PGJ$_2$ enhanced the apoptosis induced by TNF-related apoptosis-inducing ligands (TRAIL), which was not blocked by a PPARγ inhibitor [43]. In another study,15d-PGJ$_2$ significantly reduced
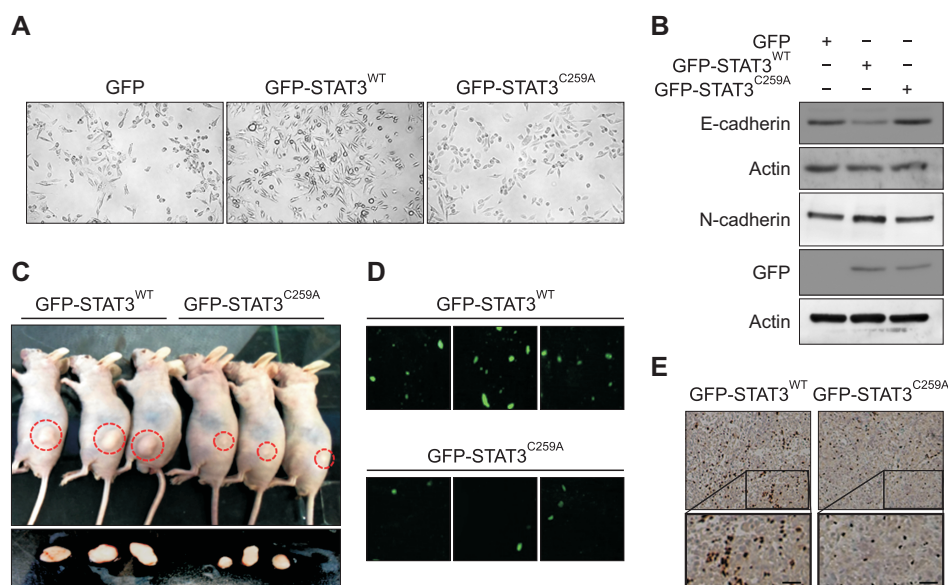

Figure 5. Effects of C259A mutation on growth and tumorigenicity of PC-3 cells. (A) Morphology of PC-3 cells transiently transfected with green fluorescent protein (GFP)-tagged STAT3^{WT} or GFP-tagged STAT3^{C259A} under phase contrast microscope. (B) Western blots of E-cadherin and N-cadherin for PC-3 cells transfected with GFP-tagged (STAT3^{WT}) or GFP-tagged (STAT3^{C259A}). (C) Effect of Cys259 mutation of STAT3 on tumor growth in a xenograft tumor model. Human PC-3 cells were transfected with GFP-tagged STAT3^{WT} or GFP-tagged STAT3^{C259A}, and 1 × 10^7 cells were injected subcutaneously into BALB/c nude mice (n = 3 per group). (D) Representative fluorescence microscopy images of GFP-GFP-STAT3^{WT} versus GFP-STAT3^{C259A} overexpressing xenografted tumor. Cells were fixed with 4% paraformaldehyde and stained for GFP antibody and detected by fluorescence. Magnification: ×20. (E) Immunohistochemistry was conducted to measure the comparative expression of P-STAT3^{Y705} in STAT3^{WT} and STAT3^{C259A} overexpressing xenograft tumor. Scale bar, 200 μm. GFP, green fluorescent protein.

the growth of oral squamous cell carcinoma, which was mainly attributed to the induction of apoptosis [44]. Under the same experimental conditions, rosiglitazone and ciglitazone, two prototypic PPARγ activators, failed to exert a growth inhibitory effect [44]. 15d-PGJ$_2$ was shown to inhibit the migrative ability of mouse mammary adenocarcinoma cells, and these effects were independent of PPARγ [42]. 15d-PGJ$_2$ can also affect the activities/expression of some redox-sensitive transcription factors such as NF-κB [6,7], AP-1 [8], STAT [44,45], p53 [46], HIF-1α [47], and Nrf2 [48] as well as their regulators, independently of PPARγ activation.

The role for the IL-6/STAT3 axis in tumor growth and progression as well as tumor-promoting inflammation has been well documented [49]. Persistent activation of IL-6/STAT3 signaling is involved in various inflammation-associated malignancies, especially, breast cancer [45,50]. Thus, aberrant overactivation of STAT3 increases cancer cell proliferation, survival, and invasion while it represses antitumor immunity [45]. Herein, we investigated whether anti-tumor effects of 15d-PGJ$_2$ could be mediated by targeting STAT3 in breast cancer cells. 15d-PGJ$_2$ treatment induced the apoptosis as evidenced by production of cleaved PARP in MDA-MB-231 and MDA-MB-468 cells with constitutively activated STAT3, but only weakly in ER-positive MCF-7 cells. In parallel with induction of apoptosis, phosphorylation of STAT3 Tyr705

was reduced in MDA-MB-231 and MDA-MB-468 cells in the presence of 15d-PGJ$_2$. These results suggest P-STAT3 as the Achilles' heel of ER-negative breast cancer. Likewise, 15d-PGJ$_2$, but not rosiglitazone and ciglitazone, inhibited STAT3 phosphorylation and induced apoptosis in human oral squamous cell carcinoma cells [44].

Many studies have shown that 15d-PGJ$_2$ structurally modifies the redox-sensitive transcriptional factors and thereby affects their functions through alkylation of cysteinyl thiol groups [51]. Canonical STAT3 activation relies on the phosphorylation of Tyr705 by JAKs, which facilitates the SH2 domain-mediated STAT3 dimerization. However, the coiled-coil domain is also considered important for dimerization and subsequent nuclear translocation of STAT3 [52-55]. Two cysteine residues (Cys251 and Cys259) located in the coiled-coil domain appear to be involved in STAT3 dimerization via disulfide linkage [36]. Computer-based docking analysis suggested Cys251 or Cys259 as putative binding sites of 15-PGJ$_2$ on STAT3. To test the validity of this in silico prediction, we conducted site-directed mutagenesis studies in which the aforementioned cysteines were replaced by alanine. PC-3 cells were transfected with wild type or cysteine 251- or 259-mutated STAT3 followed by treatment with 15-PGJ$_2$. The result shows that C259A mutation markedly attenuated the 15d-PGJ$_2$-induced apoptosis, but C251A mutation had a mar-
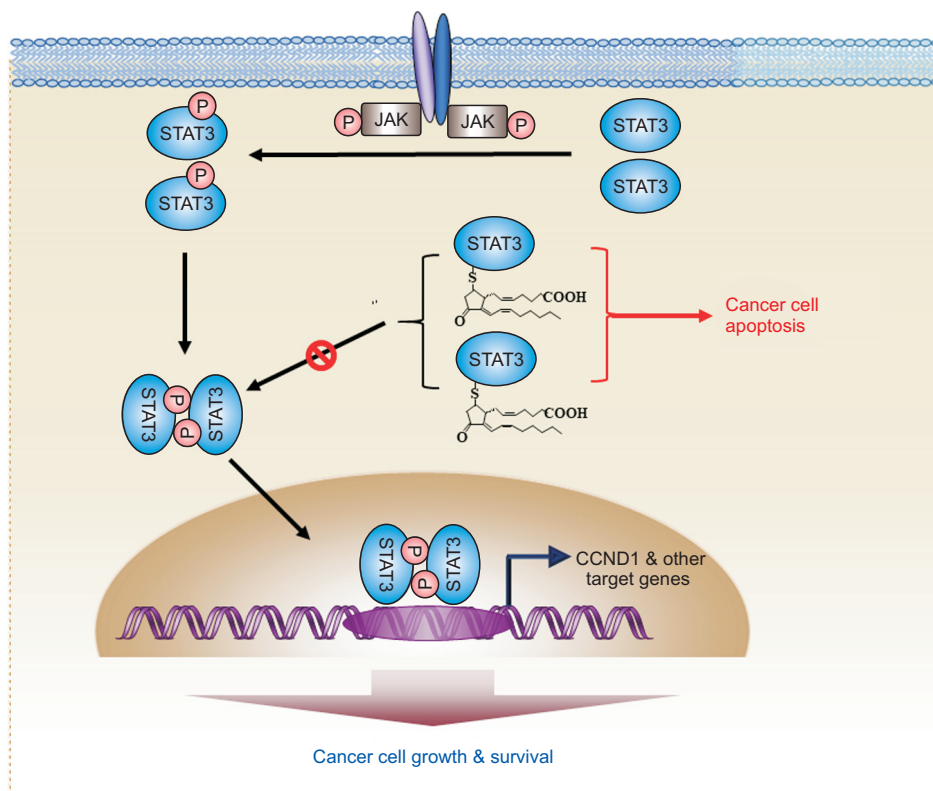

Figure 6. A proposed mechanism underlying suppression of STAT3 signaling and growth and progression of breast cancer by 15-deoxy-Δ^{12,14}-prostaglandin J$_2$ (15d-PGJ$_2$). P, phosphorylation; JAK, Janus kinase.

ginal effect. This is in agreement with our recent finding that 15d-PGJ$_2$ covalently modify Cys259 of human recombinant STAT3 as analyzed by mass spectrometry [30].

Until now, several thiol modifiers have been reported to inhibit STAT3 activity and functions. Stattic, alkylates Cys251, Cys259, Cys367, and Cys426 in STAT3 [56]. The CDDO-Me inhibits STAT3 dimerization by binding to Cys259 [57]. S3I-201 non-specifically modifies five cysteines (Cys108, Cys259, Cys367, Cys542, and Cys687) in the STAT3 protein [58]. Furthermore, 15-keto-PGE$_2$ interacts directly with Cys251 and Cys259 [59]. Notably, mutation of STAT3 Cys259 significantly retarded the growth of PC-3 prostate cancer cells, which resembles an effect achieved by covalent modification of the same amino acid by 15d-PGJ$_2$ [60].

Intensive efforts have been devoted to developing STAT3 inhibitors as anti-cancer drugs. There are two strategies for inhibiting the STAT3 signaling pathway. One approach would be targeting an upstream kinase responsible for STAT3 activation. Although the STAT3 pathway can be effectively suppressed by pharmacologic inhibition of JAK, JAK inhibitors have limitations often encountered in clinical trials, including off-target toxicities. Direct inactivation of STAT3 is less likely to cause unintentional inhibition of additional signaling pathways than targeting upstream molecules. In conclusion, the present study provides compelling evidence that 15d-PGJ$_2$ is a potential compound capable of directly antagonizing STAT3 though covalent modification of this transcription factor (Fig. 6). Therefore, 15d-PGJ$_2$ hence has a therapeutic value for the treatment of breast cancer presenting aberrant STAT3 regulation.

ACKNOWLEDGMENTS

CONFLICTS OF INTEREST

No potential conflicts of interest were disclosed.

ORCID

Su-Jung Kim, https://orcid.org/0000-0002-3636-0644
Nam-Chul Cho, https://orcid.org/0000-0002-6735-1302
Young-Il Hahn, https://orcid.org/0000-0003-2903-9251
Seong Hoon Kim, https://orcid.org/0000-0002-6573-9071
Xizhu Fang, https://orcid.org/0000-0001-6926-6614
Young-Joon Surh, https://orcid.org/0000-0001-8310-1795

REFERENCES

1. Bray F, Ferlay J, Soerjomataram I, Siegel RL, Torre LA, Jemal A. Global cancer statistics 2018: GLOBOCAN estimates of incidence and mortality worldwide for 36 cancers in 185 countries. CA Cancer J Clin 2018;68:394-424.
2. Allemani C, Weir HK, Carreira H, Harewood R, Spika D, Wang XS, et al. Global surveillance of cancer survival 1995-2009: analysis of individual data for 25,676,887 patients from 279 population-based registries in 67 countries (CONCORD-2). Lancet 2015;385:977-1010.
3. Chia S, Swain SM, Byrd DR, Mankoff DA. Locally advanced and inflammatory breast cancer. J Clin Oncol 2008;26:786-90.
4. Forman BM, Tontonoz P, Chen J, Brun RP, Spiegelman BM, Evans RM. 15-Deoxy-delta 12, 14-prostaglandin J2 is a ligand for the adipocyte determination factor PPAR gamma. Cell 1995;83:803-12.
5. Kliewer SA, Lenhard JM, Willson TM, Patel I, Morris DC, Lehmann JM. A prostaglandin J2 metabolite binds peroxisome proliferator-activated receptor gamma and promotes adipocyte differentiation. Cell 1995;83:813-9.
6. Rossi A, Kapahi P, Natoli G, Takahashi T, Chen Y, Karin M, et al. Anti-inflammatory cyclopentenone prostaglandins are direct inhibitors of IkappaB kinase. Nature 2000;403:103-8.
7. Cernuda-Morollón E, Pineda-Molina E, Cañada FJ, Pérez-Sala D. 15-Deoxy-Delta 12,14-prostaglandin J2 inhibition of NF-kappaB-DNA binding through covalent modification of the p50 subunit. J Biol Chem 2001;276:35530-6.
8. Pérez-Sala D, Cernuda-Morollón E, Cañada FJ. Molecular basis for the direct inhibition of AP-1 DNA binding by 15-deoxy-Delta 12,14-prostaglandin J2. J Biol Chem 2003;278:51251-60.
9. Shibata T, Yamada T, Ishii T, Kumazawa S, Nakamura H, Masutani H, et al. Thioredoxin as a molecular target of cyclopentenone prostaglandins. J Biol Chem 2003;278:26046-54.
10. Campbell IL. Cytokine-mediated inflammation, tumorigenesis, and disease-associated JAK/STAT/SOCS signaling circuits in the CNS. Brain Res Brain Res Rev 2005;48:166-77.
11. Furtek SL, Backos DS, Matheson CJ, Reigan P. Strategies and approaches of targeting STAT3 for cancer treatment. ACS Chem Biol 2016;11:308-18.
12. Kortylewski M, Yu H. Stat3 as a potential target for cancer immunotherapy. J Immunother 2007;30:131-9.
13. Kortylewski M, Yu H. Role of Stat3 in suppressing anti-tumor immunity. Curr Opin Immunol 2008;20:228-33.
14. Bowman T, Garcia R, Turkson J, Jove R. STATs in oncogenesis. Oncogene 2000;19:2474-88.
15. Darnell JE. Validating Stat3 in cancer therapy. Nat Med 2005;11:595-6.
16. Kunigal S, Lakka SS, Sodadasu PK, Estes N, Rao JS. Stat3-siRNA induces Fas-mediated apoptosis in vitro and in vivo in breast cancer. Int J Oncol 2009;34:1209-20.
17. Gritsko T, Williams A, Turkson J, Kaneko S, Bowman T, Huang M, et al. Persistent activation of stat3 signaling induces survivin gene expression and confers resistance to apoptosis in human breast cancer cells. Clin Cancer Res 2006;12:11-9.
18. Sarraf P, Mueller E, Jones D, King FJ, DeAngelo DJ, Partridge

JB, et al. Differentiation and reversal of malignant changes in colon cancer through PPARgamma. Nat Med 1998;4:1046-52.

19. Kubota T, Koshizuka K, Williamson EA, Asou H, Said JW, Holden S, et al. Ligand for peroxisome proliferator-activated receptor gamma (troglitazone) has potent antitumor effect against human prostate cancer both in vitro and in vivo. Cancer Res 1998;58:3344-52.

20. Elstner E, Müller C, Koshizuka K, Williamson EA, Park D, Asou H, et al. Ligands for peroxisome proliferator-activated receptorgamma and retinoic acid receptor inhibit growth and induce apoptosis of human breast cancer cells in vitro and in BNX mice. Proc Natl Acad Sci USA 1998;95:8806-11.

21. Shin SW, Seo CY, Han H, Han JY, Jeong JS, Kwak JY, et al. 15d-PGJ2 induces apoptosis by reactive oxygen species-mediated inactivation of Akt in leukemia and colorectal cancer cells and shows in vivo antitumor activity. Clin Cancer Res 2009;15:5414-25.

22. Ciucci A, Gianferretti P, Piva R, Guyot T, Snape TJ, Roberts SM, et al. Induction of apoptosis in estrogen receptor-negative breast cancer cells by natural and synthetic cyclopentenones: role of the IκB kinase/nuclear factor-κB pathway. Mol Pharmacol 2006;70:1812-21.

23. Chen YX, Zhong XY, Qin YF, Bing W, He LZ. 15d-PGJ2 inhibits cell growth and induces apoptosis of MCG-803 human gastric cancer cell line. World J Gastroenterol 2003;9:2149-53.

24. Sperandio M, Demasi APD, Martinez EF, Saad SO, Pericole FV, Vieira KP, et al. 15d-PGJ2 as an endoplasmic reticulum stress manipulator in multiple myeloma in vitro and in vivo. Exp Mol Pathol 2017;102:434-45.

25. Chinetti G, Griglio S, Antonucci M, Torra IP, Delerive P, Majd Z, et al. Activation of proliferator-activated receptors alpha and gamma induces apoptosis of human monocyte-derived macrophages. J Biol Chem 1998;273:25573-80.

26. Altiok S, Xu M, Spiegelman BM. PPARgamma induces cell cycle withdrawal: inhibition of E2F/DP DNA-binding activity via down-regulation of PP2A. Genes Dev 1997;11:1987-98.

27. Bishop-Bailey D, Hla T. Endothelial cell apoptosis induced by the peroxisome proliferator-activated receptor (PPAR) ligand 15-deoxy-Delta12, 14-prostaglandin J2. J Biol Chem 1999;274:17042-8.

28. Trindade-da-Silva CA, Reis CF, Vecchi L, Napimoga MH, Sperandio M, Matias Colombo BF, et al. 15-Deoxy-Δ(12,14)-prostaglandin J2 induces apoptosis and upregulates SOCS3 in human thyroid cancer cells. PPAR Res 2016;2016:4106297.

29. Park EJ, Park SY, Joe EH, Jou I. 15d-PGJ2 and rosiglitazone suppress Janus kinase-STAT inflammatory signaling through induction of suppressor of cytokine signaling 1 (SOCS1) and SOCS3 in glia. J Biol Chem 2003;278:14747-52.

30. Kim SJ, Cho NC, Han B, Kim K, Hahn YI, Kim KP, et al. 15-Deoxy-$\Delta^{12,14}$-prostaglandin J$_2$ binds and inactivates STAT3 via covalent modification of cysteine 259 in H-Ras-transformed human breast epithelial cells. FEBS Lett 2021;595:604-22.

31. Becker S, Groner B, Müller CW. Three-dimensional structure of the Stat3beta homodimer bound to DNA. Nature 1998;394:145-

51.

32. Bernstein FC, Koetzle TF, Williams GJ, Meyer EF Jr, Brice MD, Rodgers JR, et al. The Protein Data Bank. A computer-based archival file for macromolecular structures. Eur J Biochem 1977;80:319-24.

33. Colaprico A, Silva TC, Olsen C, Garofano L, Cava C, Garolini D, et al. TCGAbiolinks: an R/Bioconductor package for integrative analysis of TCGA data. Nucleic Acids Res 2016;44:e71.

34. Ryan AJ, Chen BB, Vennalaganti PR, Henderson FC, Tephly LA, Carter AB, et al. 15-deoxy-Delta12,14-prostaglandin J2 impairs phosphatidylcholine synthesis and induces nuclear accumulation of thiol-modified cytidylyltransferase. J Biol Chem 2008;283:24628-40.

35. Zhang T, Kee WH, Seow KT, Fung W, Cao X. The coiled-coil domain of Stat3 is essential for its SH2 domain-mediated receptor binding and subsequent activation induced by epidermal growth factor and interleukin-6. Mol Cell Biol 2000;20:7132-9.

36. Li L, Shaw PE. A STAT3 dimer formed by inter-chain disulphide bridging during oxidative stress. Biochem Biophys Res Commun 2004;322:1005-11.

37. Zhang X, Wrzeszczynska MH, Horvath CM, Darnell JE Jr. Interacting regions in Stat3 and c-Jun that participate in cooperative transcriptional activation. Mol Cell Biol 1999;19:7138-46.

38. Thiery JP, Acloque H, Huang RY, Nieto MA. Epithelial-mesenchymal transitions in development and disease. Cell 2009;139:871-90.

39. Kalluri R. EMT: when epithelial cells decide to become mesenchymal-like cells. J Clin Invest 2009;119:1417-9.

40. Quaggin SE, Kapus A. Scar wars: mapping the fate of epithelial-mesenchymal-myofibroblast transition. Kidney Int 2011;80:41-50.

41. Jin W. Role of JAK/STAT3 signaling in the regulation of metastasis, the transition of cancer stem cells, and chemoresistance of cancer by epithelial-mesenchymal transition. Cells 2020;9:217.

42. Diers AR, Dranka BP, Ricart KC, Oh JY, Johnson MS, Zhou F, et al. Modulation of mammary cancer cell migration by 15-deoxy-delta(12,14)-prostaglandin J(2): implications for anti-metastatic therapy. Biochem J 2010;430:69-78.

43. Han H, Shin SW, Seo CY, Kwon HC, Han JY, Kim IH, et al. 15-Deoxy-delta 12,14-prostaglandin J2 (15d-PGJ 2) sensitizes human leukemic HL-60 cells to tumor necrosis factor-related apoptosis-inducing ligand (TRAIL)-induced apoptosis through Akt downregulation. Apoptosis 2007;12:2101-14.

44. Nikitakis NG, Siavash H, Hebert C, Reynolds MA, Hamburger AW, Sauk JJ. 15-PGJ2, but not thiazolidinediones, inhibits cell growth, induces apoptosis, and causes downregulation of Stat3 in human oral SCCa cells. Br J Cancer 2002;87:1396-403.

45. Siersbæk R, Scabia V, Nagarajan S, Chernukhin I, Papachristou EK, Broome R, et al. IL6/STAT3 signaling hijacks estrogen receptor α enhancers to drive breast cancer metastasis. Cancer Cell 2020;38:412-23.e9.

46. Kim DH, Kim EH, Na HK, Sun Y, Surh YJ. 15-Deoxy-Delta(12,14)-prostaglandin J(2) stabilizes, but functionally

inactivates p53 by binding to the cysteine 277 residue. Oncogene 2010;29:2560-76.

47. Choi JE, Kim JH, Song NY, Suh J, Kim DH, Kim SJ, et al. 15-Deoxy-$\Delta^{12,14}$-prostaglandin J$_2$ stabilizes hypoxia inducible factor-1α through induction of heme oxygenase-1 and direct modification ofprolyl-4-hydroxylase 2. Free Radic Res 2016;50:1140-52.

48. Kim EH, Kim SJ, Na HK, Han W, Kim NJ, Suh YG, et al. 15-Deoxy-$\Delta^{12,14}$-prostaglandin J$_2$ upregulates VEGF expression via NRF2 and heme oxygenase-1 in human breast cancer cells. Cells 2021;10:526.

49. Yu H, Kortylewski M, Pardoll D. Crosstalk between cancer and immune cells: role of STAT3 in the tumour microenvironment. Nat Rev Immunol 2007;7:41-51.

50. Wang N, Wei L, Huang Y, Wu Y, Su M, Pang X, et al. miR520c blocks EMT progression of human breast cancer cells by repressing STAT3. Oncol Rep 2017;37:1537-44.

51. Kim EH, Surh YJ. 15-deoxy-Delta12,14-prostaglandin J2 as a potential endogenous regulator of redox-sensitive transcription factors. Biochem Pharmacol 2006;72:1516-28.

52. Ma J, Zhang T, Novotny-Diermayr V, Tan AL, Cao X. A novel sequence in the coiled-coil domain of Stat3 essential for its nuclear translocation. J Biol Chem 2003;278:29252-60.

53. Sato N, Tsuruma R, Imoto S, Sekine Y, Muromoto R, Sugiyama K, et al. Nuclear retention of STAT3 through the coiled-coil domain regulates its activity. Biochem Biophys Res Commun 2005;336:617-24.

54. Ma J, Cao X. Regulation of Stat3 nuclear import by importin alpha5 and importin alpha7 via two different functional sequence elements. Cell Signal 2006;18:1117-26.

55. Horvath CM, Stark GR, Kerr IM, Darnell JE Jr. Interactions between STAT and non-STAT proteins in the interferon-stimulated gene factor 3 transcription complex. Mol Cell Biol 1996;16:6957-64.

56. Heidelberger S, Zinzalla G, Antonow D, Essex S, Basu BP, Palmer J, et al. Investigation of the protein alkylation sites of the STAT3:STAT3 inhibitor Stattic by mass spectrometry. Bioorg Med Chem Lett 2013;23:4719-22.

57. Ahmad R, Raina D, Meyer C, Kufe D. Triterpenoid CDDO-methyl ester inhibits the Janus-activated kinase-1 (JAK1)-->signal transducer and activator of transcription-3 (STAT3) pathway by direct inhibition of JAK1 and STAT3. Cancer Res 2008;68:2920-6.

58. Ball DP, Lewis AM, Williams D, Resetca D, Wilson DJ, Gunning PT. Signal transducer and activator of transcription 3 (STAT3) inhibitor, S3I-201, acts as a potent and non-selective alkylating agent. Oncotarget 2016;7:20669-79.

59. Lee EJ, Kim SJ, Hahn YI, Yoon HJ, Han B, Kim K, et al. 15-Keto prostaglandin E$_2$ suppresses STAT3 signaling and inhibits breast cancer cell growth and progression. Redox Biol 2019;23:101175.

60. Kim SJ, Saeidi S, Cho NC, Kim SH, Lee HB, Han W, et al. Interaction of Nrf2 with dimeric STAT3 induces IL-23 expression: implications for breast cancer progression. Cancer Lett 2021;500:147-60.